Neurological Sciences (2019) 40:2479–2489
https://doi.org/10.1007/s10072-019-04014-y

REVIEW ARTICLE

# The diagnostic value of SNpc using NM-MRI in Parkinson's disease: meta-analysis

Xiangming Wang[1] · Yuehui Zhang[1] · Chen Zhu[1] · Guangzong Li[1] · Jie Kang[1] · Fang Chen[1] · Ling Yang[1]

Received: 11 February 2019 / Accepted: 16 July 2019 / Published online: 7 August 2019


## Abstract

The main purpose of this study was to systematically evaluate the accuracy of neuromelanin-sensitive magnetic resonance imaging (NM-MRI) in Parkinson's disease (PD) diagnosis using a meta-analysis method. In PubMed, Web of Science, Embase, and Google Scholar, the literatures were searched for the diagnostic value of neuromelanin-sensitive magnetic resonance imaging in PD. The literatures were screened in the light of Preferred Reporting Items for Systematic Reviews and Meta-Analyses (PRISMA). Data analysis was processed by Stata 12.0 software to obtain meta-analysis, heterogeneity analysis, and publication bias. Meta-analysis results showed by using NM-MRI observed substantia nigra pars compacta (SNpc) on PD, the pooled diagnostic sensitivity and specificity were 0.82 (95% CI, 0.74–0.87) and 0.82 (95% CI, 0.73–0.89), respectively. And the pooled positive likelihood ratio (PLR) and negative likelihood ratio (NLR) were 4.58 (95% CI, 3.08–6.82) and 0.22 (95% CI, 0.16–0.31), respectively. Moreover, subgroup analysis according to the measurement criteria of SNpc showed the SNpc volume should be used as good a marker for diagnosing PD. Finally, Fagan test demonstrated that when PLR was equal to 5, the posterior probability is significantly enhanced to 53%, compared with prior probability (20%). As for NLR (0.22), the prior probability is 20%, while the posterior probability remarkably dropped to 5%. In conclusion, SNpc signal detected by NM-MRI exhibited high sensitivity and specificity for diagnosis of PD, which was a high-performance imaging diagnostic method for PD. We recommend NM-MRI imaging technology to be widely used in Parkinson's diagnosis.

**Keywords** Parkinson's disease · Neuromelanin-sensitive magnetic resonance imaging (NM-MRI) · Meta-analysis · Diagnostic method

✉ Ling Yang
e089761@163.com

Xiangming Wang
zsmvof8@163.com

Yuehui Zhang
zgi6911@163.com

Chen Zhu
rqxbn98@163.com

Guangzong Li
lf57171@163.com

Jie Kang
etno114@163.com

Fang Chen
my54126@163.com

[1] Department of Neurology, Panzhihua Central Hospital, No. 34 Yikang Street, Panzhihua City 617067, Sichuan Province, People's Republic of China

## Introduction

Idiopathic Parkinson's disease, a common global chronic neurological disease, is the second largest neurological disease after Alzheimer's disease [1]. With the development of society, the number of patients with Parkinson's disease is increasing. According to statistics, the number of Parkinson's disease patients in China has reached to 200 million currently [2]. World Health Organization experts predict that the number of Parkinson's patients in China will reach 5 million in 2030 [3]. Parkinson's disease (PD) is a chronic progressive disease, whose clinical manifestations include progressive aggravation of exercise retardation, myotonia, resting tremor, and posture gait balance disorder [4]. Neuropathological changes mainly exhibit degeneration of neuromedin-containing neurons in the substantia nigra pars compacta (SNpc) [5, 6]. Neuromelanin is an important intermediate in the synthesis of dopamine and norepinephrine by neurons, so they can be observed in the substantia nigra pars compacta (SNpc) and locus coeruleus

(LC) [7, 8]. And the content of melanin is correlated with the number of dopamine and norepinephrine neurons. The early symptoms of Parkinson's disease are not typical, and the diagnosis is difficult [9]. When the motor symptoms are present, the disease has progressed to the middle and late stages [10], which has a significant impact on the daily life and work of the patients. Therefore, early diagnosis and timely intervention will improve the efficacy of treatment and life quality of patients [11]. The diagnosis of Parkinson's disease (PD) relies on clinical symptoms, signs, Parkinson's test scale, and levodopa test [12–15]. Magnetic resonance imaging (MRI) is considered a valuable tool for diagnosis of cerebral disease [16, 17]. Razek et al. [18] found that apparent diffusion coefficient (ADC) value measured by MRI is a promising parameter for predication of effect of levodopa on brain parenchyma in patients with PD. However, traditional MRI techniques have failed to depict neuromelanin-containing nuclei such as the SNc and LC [19].

In recent years, with the development of melanin-sensitive sequence, neuromelanin-sensitive MRI (NM-MRI) imaging technology is gradually applied to the diagnosis of Parkinson's disease (PD) [20]. The neuromelanin-sensitive sequence was first proposed to visualize the melanin in the substantia nigra and the blue spot by Sasaki et al. in 2006 [19]. Neuromelanin-sensitive MRI (NM-MRI) imaging is based on the paramagnetic properties of chelated metals of neuromelanin (NM) [19, 21]. High-resolution fast spin echo (FSE) T1WI images obtained at 3 T can capture the neuromelanin-generated signals from these nuclei by virtue of the synergic effects of high signal-to-noise ratio, high spatial resolution, signal suppression of the surrounding brain tissue by T1 prolongation at a high magnetic field, and magnetization transfer effect during multi-slice FSE acquisition [22]. In 2006, Sasaki's team began using NM-MRI to successfully display normal and abnormal midbrain substantia nigra and blue plaques [19]. This imaging technique uses a 3-T high-resolution fast spin echo T1-weighted sequence [23]. Some studies have used NM-MRI techniques to demonstrate the diagnosis of PD by measuring the signal intensity, volume or area of SNpc, and locus coeruleus (LC) structures. Matsuura et al. [24] applied NM-MRI into a patient with PD to investigate possible alterations of these catecholaminergic neurons. The contrast ratio of the SNc was decreased in PD patients. Also, the contrast ratio of the SNc was correlated with the Hoehn-Yahr stage of PD. The study of Prasad et al. found that the neuromelanin sequence contrast ratio of the central and lateral SNc was significantly lower in patients with PD, which is also correlated with the scores of Unified Parkinson's Disease Rating Scale-III OFF state [25]. Schwarz et al. [26] believed that reduction of normalized neuromelanin volume in PD was most pronounced in the posterior SNpc, followed by the anterior SNpc and the LC. NM-MRI exhibits a kind of high diagnostic accuracy method for PD, which is also associated with disease severity. The diagnostic accuracy of the NM-MRI technology in PD needs to be explored by the meta-analysis of comprehensive data. More details of application of NM-MRI into PD should be explored. The primary objective of this study was to evaluate the diagnostic utility of NM-MRI in PD by meta-analysis method, to further explore the application of NM-MRI into PD.

## Materials and methods

### Study inclusion and exclusion criteria

The study was based on Preferred Reporting Items for Systematic Reviews and Meta-Analyses (PRISMA) guidelines. When searching for English literature, "neuromelanin-sensitive magnetic resonance imaging" and "Parkinson's disease" were used as keywords, and free words are arbitrarily matched as search sentences. Then, we searched in Web of Science, PubMed, Embase, and Google academic databases and traced back secondary literature searches to prevent leak. And the retrieval deadline was June 15, 2018. EndNote X7was used to re-screen the literatures obtained from these databases (Web of Science, PubMed, Embase, and Google). The searched documents are gradually screened from the title, abstract, and full text according to the pre-set inclusion and exclusion criteria. The two researchers conducted the same discussion at the same time. When there is controversy, it should be judged by the third researcher.

Inclusion criteria are as follows: (1) use NM-MRI technology to diagnose PD by measuring the signal intensity, volume, or area of the SNpc structure; (2) have the exact sensitivity and specificity of the cutoff value, or optimal sensitivity and specificity can be obtained in the ROC curve; (3) there are clear gold standards; and (4) if the data is repeated, select the most recent published or most detailed literature.

Exclusion criteria are as follows: (1) excluding reviews, case reports, reviews, guides, letters, cell experiments, animal experiments, and simulation experiments and (2) unable to extract data exclusion.

### Literature search strategy

In order to ensure the recall rate of the search, the medical keyword and the free word search should be simultaneously used. When searching for English literature, "neuromelanin-sensitive magnetic resonance imaging" and "Parkinson's disease" were used as keywords. And free words are arbitrarily matched, when searching in Web of Science, PubMed, Embase, and Google academic databases. Also, we traced back secondary literature searches to prevent leak investigation. The retrieval deadline was set as the June 15, 2018. The

literatures from database of Web of Science, PubMed, and Embase were combined. And duplicates were screened by using EndNote X7. Furthermore, the literatures from Google academic database were checked carefully to ensure retrieval recall.

Two reviewers independently conducted a quality assessment tool for diagnostic accuracy studies (QUADAS-2). And then, the risk of publication bias and concerns regarding the applicability of studies were assessed by visually inspecting QUADAS-2 plots.

### Data extraction

The extraction was also carried out independently by two researchers. When the opinions were inconsistent, the third researcher was sought to discuss the solution. The extracted data are shown in Table 1, which included TP, TN, FP, FN, and optimum cutoff value (sensitivity and specificity). If the study did not directly give the best cutoff value, the ROC curve should be given in the paper. Engauge Digitizer 4.1 was used to intercept the last point of the ROC curve and output the sensitivity and specificity corresponding to the point. Further, the "Youden Index" (sensitivity-(1-specificity)) method was used: when the value of the Youden Index is maximum, the point is the best cutoff value.

### Risk of bias in individual studies

A Cochran-$Q$ test of heterogeneity was performed to evaluate inconsistency index ($I^2$), as a measure to illustrate the percentage of the total variability caused by heterogeneity instead of chance. A value of $I^2$ more than 50 and a $P$ value $< 0.05$ indicate evident heterogeneity. Since the cutoff values were different among the included studies, diagnostic threshold effects were inspected. The summary receiver operating curve (SROC) was visually evaluated to detect the threshold effect. And Spearman correlation analysis was used to assess the heterogeneity derived from the diagnostic threshold effects.

Deeks' funnel plot asymmetry analysis was performed to identify the publication bias. Briefly, the Deeks funnel plot was a scatter plot of the inverse of the square root of effective sample size (1/root (ESS)) against the ln (diagnostic odds ratio (DOR)).

### Data synthesis and statistical analysis

The indexes of sensitivity, specificity, positive likelihood ratio (PLR), negative likelihood ratio (NLR), DOR, odds ratios, and area under the summary receiver operating curve (AUSROC) were pooled and analyzed by meta-analysis. Furthermore, Fagan's nomogram analysis was conducted. The Fagan nomogram plot comprised three vertical axes. The left axis represents the pre-test probability, which was derived from the prevalence in each included study. Another axis in the middle displayed the likelihood ratio showing the extent to which the index could raise or lower the probability of having the disease. The right vertical axis signified the post-test probability of patient's probability of having the positive or negative results of the reference standard test. Moreover, subgroup analyses based on SNc volume were carried out. All data synthesis and most statistical analyses were undertaken by Stata software version 12.0 (College Station, TX, USA) with the corresponding 95% confidence interval (CI). The sensitivity, specificity, DOR, and AUSROC were considered the major outcomes in this study. The summary receiver operating curve (SROC) was visually evaluated at first. Furthermore, the left axis represents the pre-test probability, which was derived from the prevalence in each included study. Another axis in the middle displayed the likelihood ratio showing the extent to which the index could raise or lower the probability of having the disease. The right vertical axis signified the post-test probability of patient's probability of having the positive or negative results of the reference standard test.

All data synthesis and most statistical analyses were undertaken by Stata software version 12.0 (College Station, TX, USA).

## Results

### Characteristics of studies and data

The PRISMA flow diagram illustrated the literature selection process as shown in Fig. 1. In the light of the search strategy, 146 articles were identified from Web of Science, PubMed, and Embase databases. After screening of title and abstract and removal of duplicates, 35 articles were selected for further review. And the search strategy identified a total of 149 publications in Google Scholar. With screening of title and abstract, 29 articles were chosen for further review. Then, we combined these publications and removed the duplicates, leading to 27 articles for further study. By further reading these 27 research articles, 17 articles were eliminated based on exclusion criteria. Finally, a total of 10 studies were included in the meta-analysis.

In accordance with inclusion criteria, all studies used United Kingdom Parkinson's Disease Society Brain Bank as "gold standard." The selected studies were conducted in Japan ($n = 5$), Spain ($n = 1$), Italy ($n = 1$), Portugal ($n = 1$), India ($n = 1$), and the UK ($n = 1$). Finally, a total of 272 patients with PD who underwent NM-MRI were included in the meta-analysis. Table 1 shows the characteristics of the inclusion studies.

Further, quality of studies and risk of bias were conducted by QUADAS-2 (Table 2) and funnel plot (Fig. 2). As illustrated in Table 2, the studies presented a low to moderate risk of

**Table 1** Details of studies selected for meta-analysis

| First name | Country | Sample acquisition time | Diagnostic criteria for PD | Study design | Consecutive or random patients | Exam | SNpc analyzed measures | Treatment | The type of PD | Sample size | | Gender (male%) | | Mean age | |
|---|---|---|---|---|---|---|---|---|---|---|---|---|---|---|---|
| | | | | | | | | | | PD | Control | PD | Control | PD | Control |
| Ohtsuka et al. [33] | Japan | 2006–2010 | United Kingdom Parkinson's Disease Society Brain Bank [15] | Prospectively | Yes | NM-MRI | Signal intensity | Not received any treatment | Early/advanced PD | 30/31 | Healthy/22 | 0.47 | 0.22 | 50–78 | 60–80 |
| Taniguchi et al. [8] | Japan | 2014–2015 | International Parkinson and Movement Disorder Society | Prospectively | Yes | NM-MRI | Area, volume | – | Idiopathic PD | 24 | Healthy/10 | 0.58 | 0.5 | 72.7 ± 6.5 | 72.7 ± 2.7 |
| Castellanos et al. [35] | Spain | – | UK Brain Bank criteria | Prospectively | Yes | NM-MRI | Volume | Treatment with the UPDRS-III | Idiopathic PD | 23 | Healthy/37 | 0.78 | 0.51 | 55–70 | 52–70 |
| Takahashi et al. [36] | Japan | 2014–2016 | UK Brain Bank criteria | Prospectively | Yes | NM-MRI | Volume | – | Early PD | 18 | Healthy/18 | 0.55 | 0.55 | 71.2 ± 6.94 | 67.1 ± 4.75 |
| Isaias et al. [37] | Italy | – | United Kingdom Parkinson's Disease Society Brain Bank | Prospectively | – | NM-MRI | Volume | Not received any treatment | PD | 18 | Healthy/18 | 0.72 | 0.61 | 46–77 | 47–77 |
| Ogisu et al. [38] | Japan | 2011–2012 | United Kingdom Parkinson's Disease Society Brain Bank | Prospectively | – | NM-MRI | Volume | – | PD | 18 | Healthy/27 | 0.44 | 0.48 | 68.8 ± 6.4 | 65.9 ± 6.7 |
| Matsuura et al. [24] | Japan | – | Clinically diagnosed | – | Yes | NM-MRI | Area | – | PD | 32 | Healthy/23 | 0.71 | 0.43 | 71.4 ± 8.6 | 71.2 ± 8.9 |
| Reimao et al. [34] | Portugal | – | UK Brain Bank criteria | Prospectively | – | NM-MRI | Area | Not received any treatment | Early/advanced PD | 12/10 | Healthy/10 | – | – | 63.23 ± 11.9 | 61.2 ± 7.3 |
| Prasad et al. [25] | India | – | United Kingdom Parkinson's Disease Society Brain Bank | – | No | NM-MRI | Signal intensity | – | PD | 16 | Healthy/15 | 0.68 | 0.73 | 57.5 ± 7.89 | 56.3 ± 8.52 |
| Schwarz et al. [26] | UK | 2007–2015 | United Kingdom Parkinson's Disease Society Brain Bank | Prospectively | – | NM-MRI | Signal intensity | – | PD | 39 | Healthy/30 | 0.56 | 0.56 | 51.8–87.1 | 41.3–82.8 |

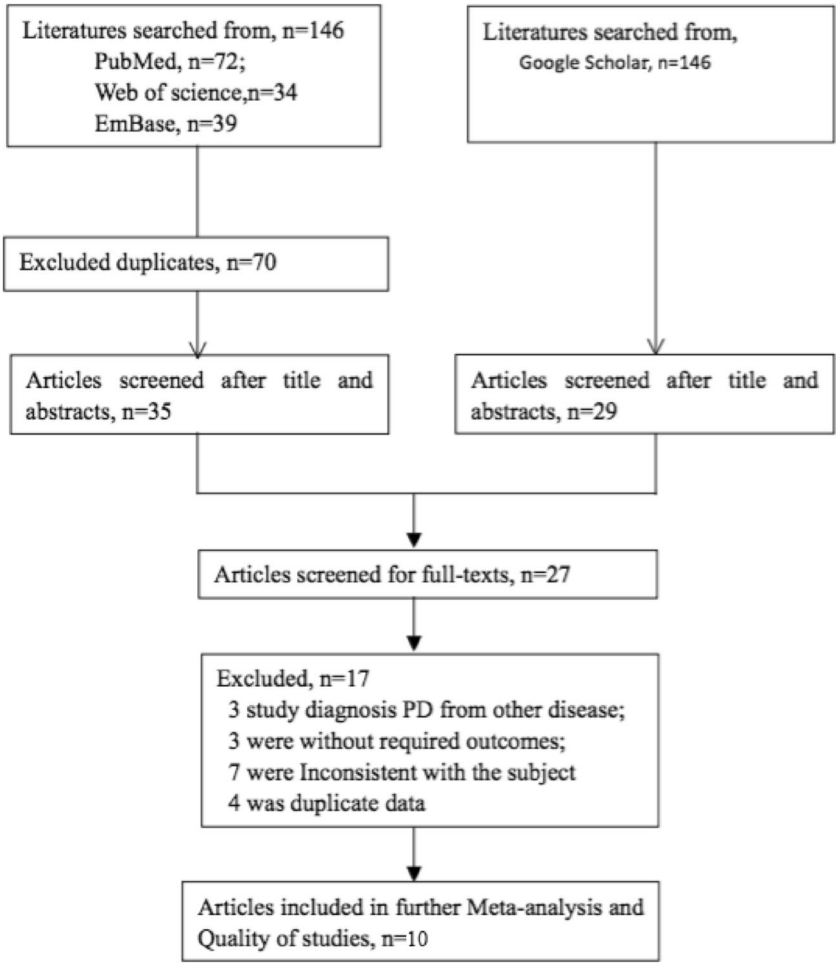


**Fig. 1** PRISMA flow diagram of the search strategy and selection of studies included in the meta-analysis

bias and low concerns about applicability. And funnel plot and the Egger test showed no evidence of publication bias (Deeks' $t$ value = − 0.70; $P = 0.496$, Fig. 2).

## Diagnostic value of SNpc for PD

All studies used the SNpc value measured by NM-MRI to diagnose PD. And the results were analyzed by the indexes of sensitivity, specificity, NLR, PLR, DOR, and odds ratio calculations. Spearman analysis results show that the correlation coefficient value is − 0.74 ($P = 0.55$), suggesting no obvious threshold effect. Therefore, the data could be combined for meta-analysis. After combining these indexes, the heterogeneity was examined. As shown in Fig. 3, it could be found that there was a certain extent of heterogeneity for the index sensitivity, specificity, NLR, PLR, and especially odds ratio, indicating the existence of heterogeneity among these indexes due to non-threshold effects. Therefore, quantitative synthesis of these indexes should use a random effects model, while for the index of DOR and PLR, there were little heterogeneity and middle heterogeneity ($I^2 = 13.5\%$ and $I^2 = 39.21\%$), respectively. So a fixed model analysis was applied into these two indexes. In bivariate analysis, final pooled sensitivity was 0.82 (95% CI, 0.74–0.87), and final pooled specificity was 0.82 (95% CI, 0.73–0.89). And the pooled PLR and NLR were 4.58 (95% CI, 3.08–6.82) and 0.22 (95% CI, 0.16–0.31), respectively. Moreover, the combined DOR and odds ratio were 3.02 (95%, CI, 2.50–3.55) and 20.56 (95% CI, 12.18–34.68), respectively. These results demonstrate that the SNpc value has good capacity to diagnose PD. Furthermore, the summary ROC curve was presented in Fig. 4. The overall accuracy of SNpc defined by NM-MRI was 89%.

## Subgroup analysis and threshold effect

There is heterogeneity of multiple research indicators in the above results, which may result from the different measurement criteria of SNpc in each study. Therefore, we conducted a subgroup analysis by different methods of SNpc. And the results show that the SNpc volume behaved as a good marker for diagnosing PD. Further, the heterogeneity among these indexes was significantly reduced in subanalysis of SNpc volume. And there was a certain increase in sensitivity and specificity: sensitivity, 0.86 (95% CI, 0.80–0.91; $I^2 = 0.00\%$);

**Table 2** QUADAS-2 assessment of included studies

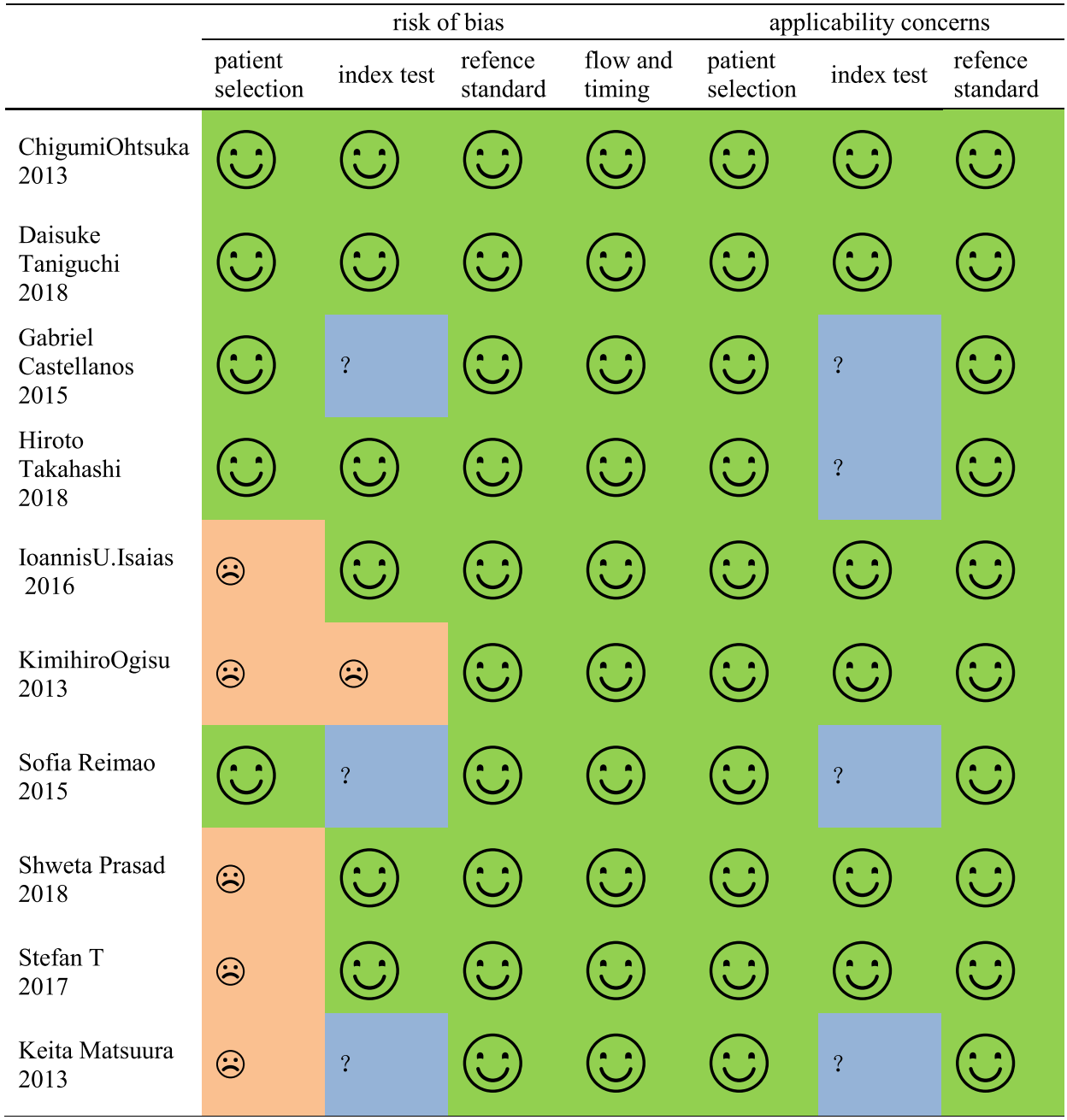


☹, high risk; ☺, low risk; ?, unclear

specificity, 0.83 (95% CI, 0.74–0.92; $I^2 = 50.43\%$). The PLR and NLR were 4.9 (95% CI, 3.2–7.5; $I^2 = 28.5\%$) and 0.18 (95% CI, 0.12–0.25; $I^2 = 0.00\%$). DOR and odds ratio were also significantly increased to 28 (95% CI, 14–56) and 27.8 (95% CI, 13.9–55.7), respectively. The area under the SAUC curve is 0.90 (95% CI, 0.87–0.92). The analysis results show that NM-MRI measurement of the SNpc volume would have higher accuracy and authenticity for diagnosis of PD.

In this meta-analysis, the SROC curve measured by NM-MRI in the SNpc region has no typical shoulder-arm profile, suggesting that there is no negative correlation between sensitivity and specificity. And the results of Spearman analysis show that the correlation coefficient is −0.74 ($P = 0.55$), prompting no significant threshold effect.

## Clinical utility test

Fagan (Fig. 5) revealed the relationship among the prior probability, likelihood ratio, and the posterior probabilities, which reflected the changes of diagnosis of PD by using NM-MRI

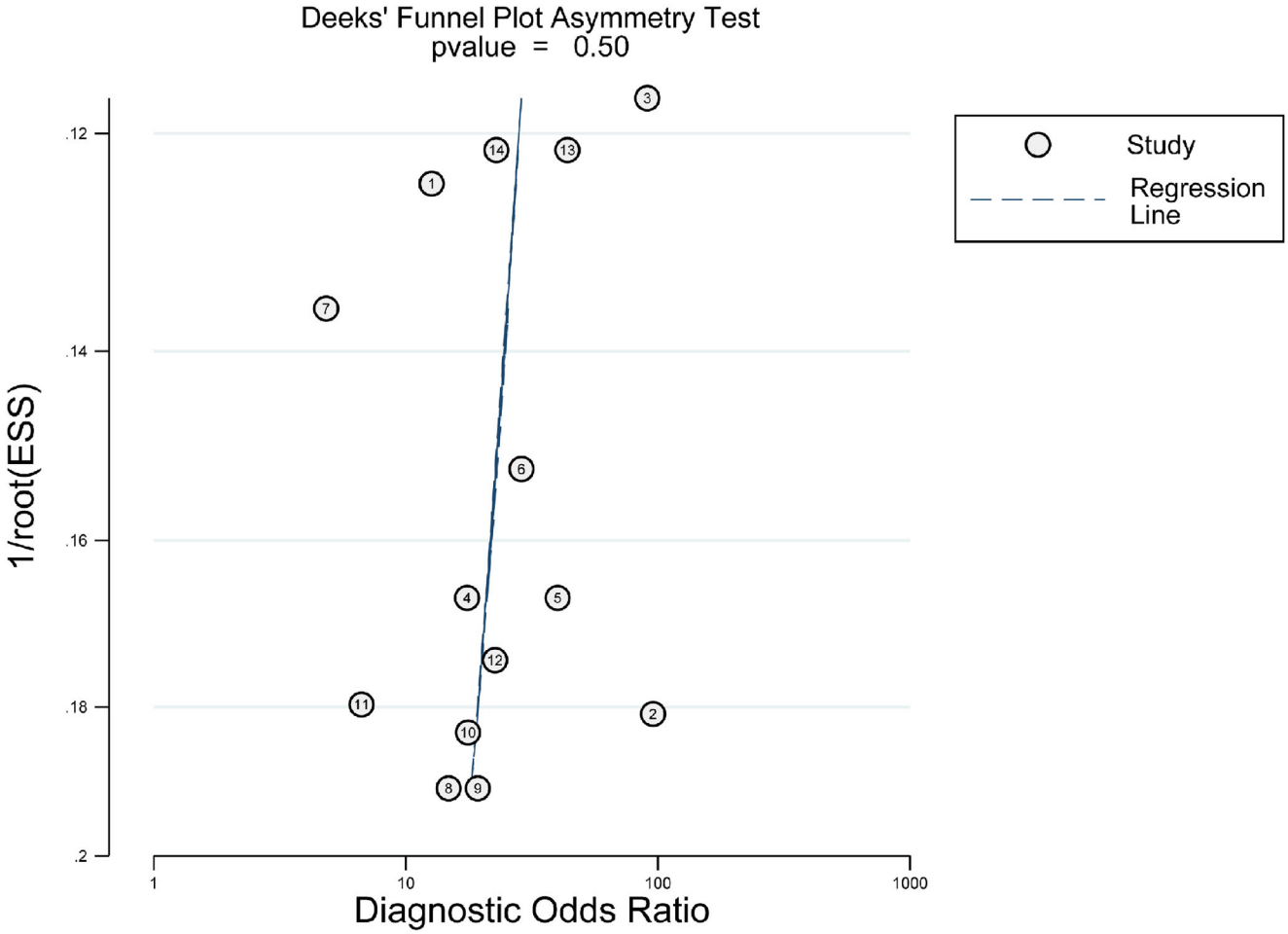


**Fig. 2** Deeks's funnel plot for the diagnostic value of using the SNpc measured by NM-MRI to define PD as normal

detection of SNpc. As shown in Fig. 5, when PLR was equal to 5, the posterior probability was evidently increased to 53% compared with the prior probability (20%). While NLR was equal to 0.22, the posterior probability significantly dropped to 5% compared with the prior probability (20%). Thus, the SNpc value detected by NM-MRI exhibited a significantly increased diagnostic efficacy.

## Discussion

As a common progressive neurodegenerative disease, the incidence of Parkinson's disease has been increasing year by year [27]. Parkinson's motor symptoms are mainly characterized by bradykinesia, myotonia, resting tremor, and posture balance disorder. The pathological changes in Parkinson's disease are the significant loss of dopaminergic neurons containing neuromelanin in the substantia nigra pars compacta, the formation of Lewy bodies in neurons and the caudate nucleus, and so on [28]. However, it is worth noting that patients with PD usually have neuropathological abnormalities before the typical symptoms occur. In patients with PD, the neuronal loss in the substantia nigra pars compacta (SNpc) usually does not show clinical motor symptoms before it reaches 80% [29]. That disease has existed until a few years or decades before the classic motor symptoms appear. So early detection of such abnormal pathological changes is conducive to timely diagnose PD and to improve the life quality of patients with PD.

The decrease of neurocytes containing neuromelanin in SNpc is a pathological marker of PD [30]. Neuromelanin is a black polymer produced by specific catecholamine neurons in the brain [31]. In early PD, neuromelanin can protect against neuronal damage by iron-mediated oxidative stress by chelation of iron [31]. As Parkinson's disease progresses, the release of neuromelanin may aggravate the autoimmune response of PD. However, we cannot detect neuronal loss by conventional magnetic resonance imaging, mainly because MRI cannot directly visualize normal or abnormal SNc and LC. In 2006, Sasaki's team [19] firstly developed NM-MRI imaging techniques, which successfully showed normal and abnormal SNc and LC in MRI images. NM-MRI imaging is based on paramagnetic properties, causing a T1 shortening effect and a high signal onT1-weighted imaging. NM-MRI imaging is evident in healthy controls, whereas in

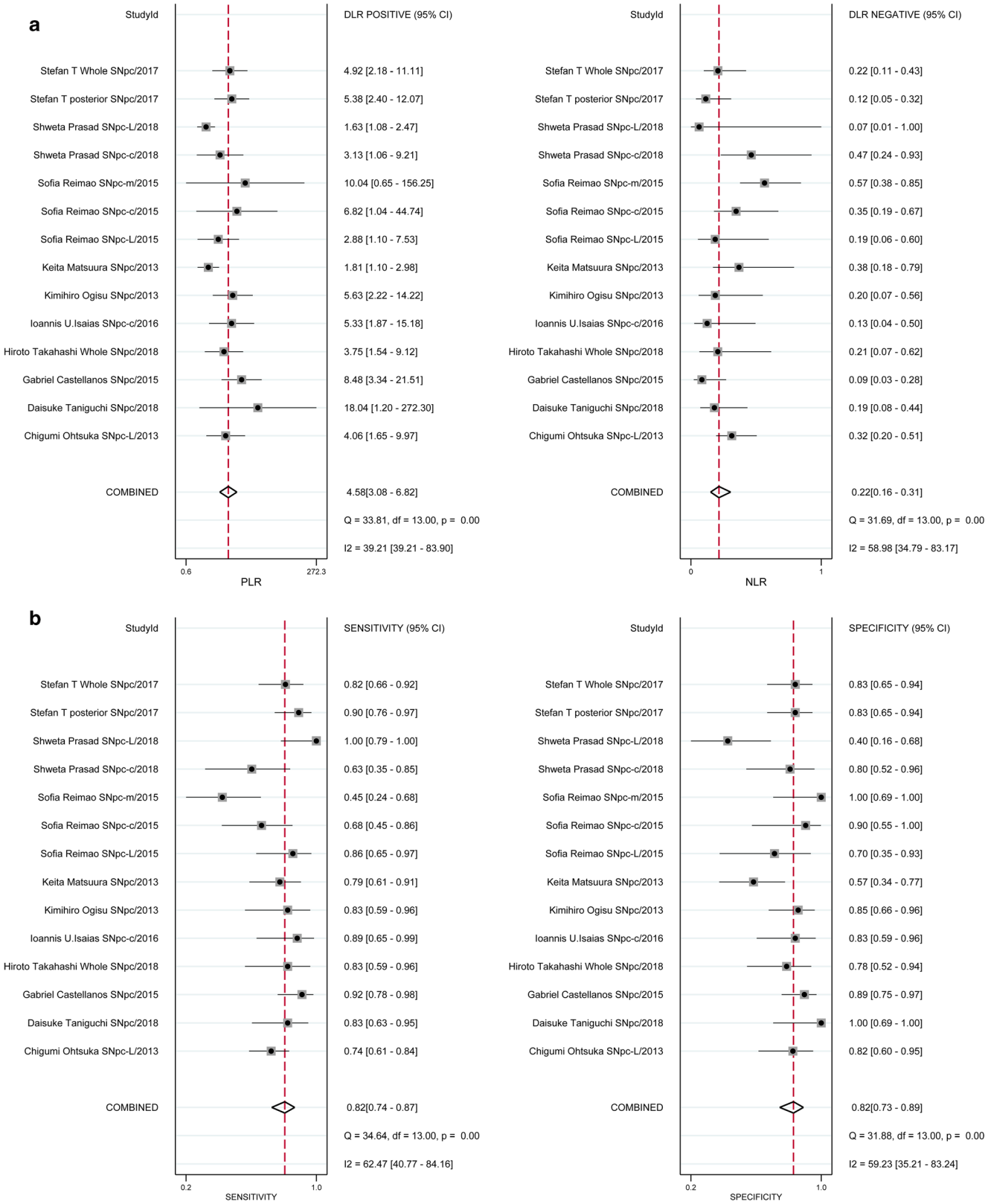


**Fig. 3** Positive likelihood ratio (**a**, left), negative likelihood ratio (**a**, right), sensitivity (**b**, left), specificity (**b**, right), diagnostic odds radio (**c**, left), odds ratio (**c**, right), and their forest plots for the diagnostic value of using the SNpc value measured by NM-MRI to define PD

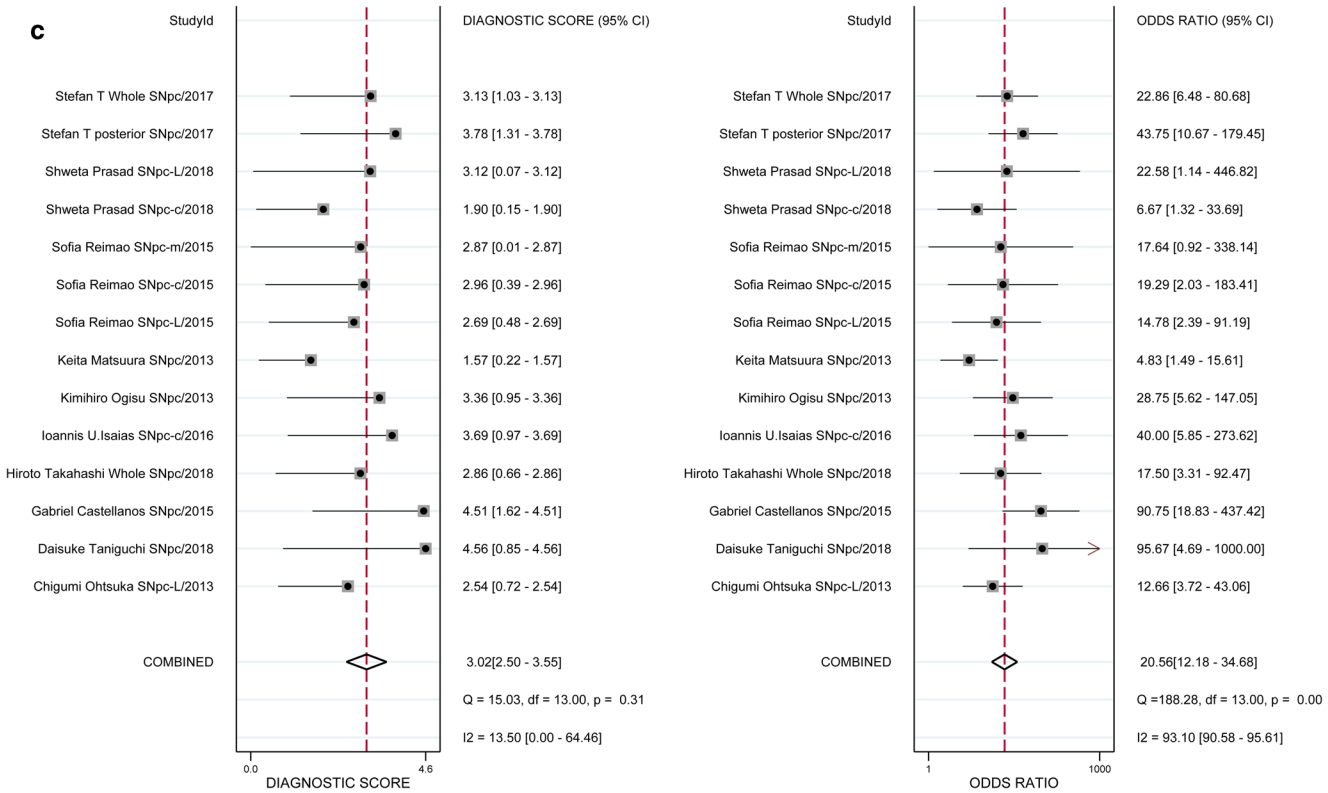


**Fig. 3** continued.

Parkinson's patients, the signal is significantly reduced, which is strongly consistent with the reduction of early pathological neuronal melanocytes in Parkinson's disease [32]. By applying NM-MRI, the searchers found that changes in SNc signals have a high sensitivity and specificity for diagnosis of

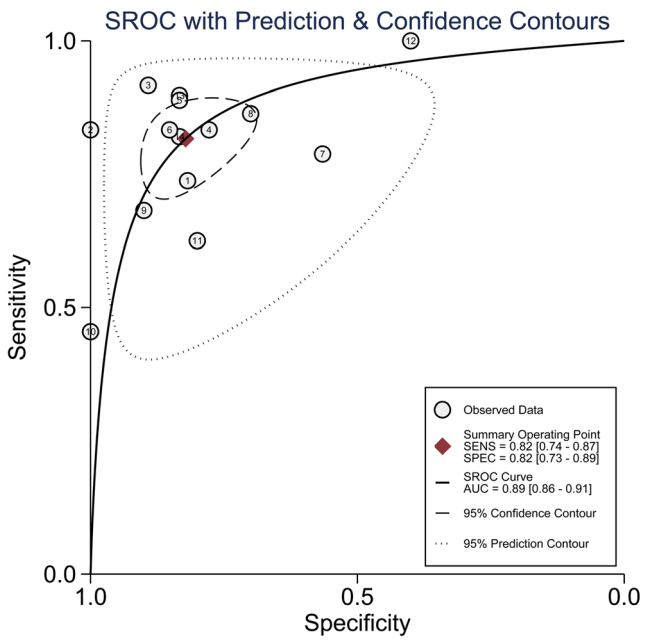


**Fig. 4** The SROC curve and AUC for the diagnostic value of using the SNpc measured by NM-MRI to define PD as normal

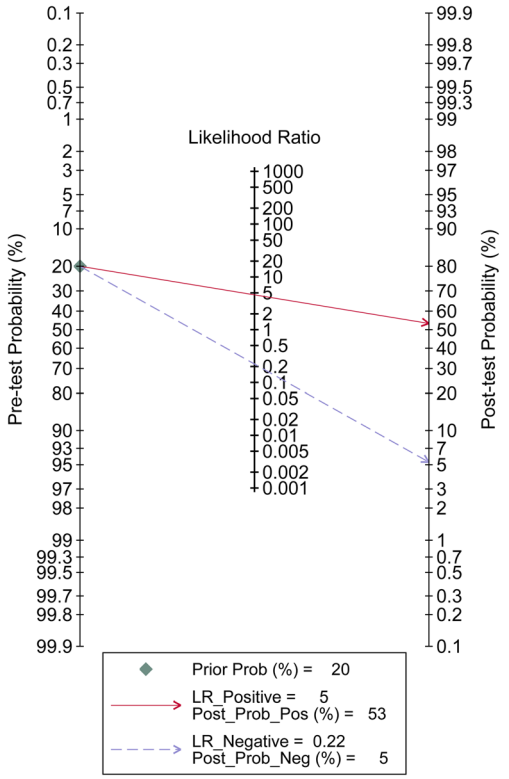


**Fig. 5** The Fagan plot for the diagnostic value of using the SNpc measured by NM-MRI to define PD as normal

Parkinson's disease. In this present study, we performed a meta-analysis to evaluate the value of SNpc detected by NM-MRI in the diagnosis of PD. The related indexes were pooled and analyzed. For index of sensitivity, specificity, NLR, and especially odds ratio, there is statistical heterogeneity due to non-threshold effects ($I > 50\%$). Therefore, quantitative synthesis of data is analyzed using a random effects model. These results demonstrate that the SNpc value has good capacity to diagnose PD. Further, the overall accuracy of SNpc defined by NM-MRI was 89%. But there was heterogeneity among these data, which may result from the different measurement criteria of SNpc in each study. For example, Prasad et al. and Ohtsuka et al. used different signal intensities of SNpc to diagnose PD [25, 33], whereas Reimao et al. used SNpc area for diagnosis of PD [34]. And the rest of the studies used SNpc volume to diagnose PD. Thus, subgroup meta-analysis was conducted, and the analysis results show that NM-MRI measurement of SNpc volume has higher accuracy and authenticity. These above results prompted us that the various ways of measurement of SNpc value by NM-MRI were adopted in different studies. It is recommended to use the SNpc volume as the best marker for diagnosing PD. This is because the substantia nigra in the brain is a three-dimensional structure. The measurement of SNpc volume by NM-MRI can more accurately reflect the substantia nigra of the midbrain and the loss of melanin in SNpc.

In summary, NM-MRI imaging technology provides a valuable test for Parkinson. However, the further application of NM-MRI imaging technology into diagnosis of Parkinson's patients is still under investigation. A large-scale sample data about application of NM-MRI imaging technology into early PD should be performed in a multi-center study. The best measurement area and the best measurement indicators of NM-MRI imaging technology to diagnose Parkinson's should be explored as well. And there are some limits in this study, such as the large variability among different studies in terms of measurements, MR study protocol, and MR data analysis limit. Therefore, we recommend the standard protocol of NM-MRI imaging technology to be widely used in Parkinson's diagnosis and look forward to more multi-center research data.

**Compliance with ethical standards** The study was based on Preferred Reporting Items for Systematic Reviews and Meta-Analyses (PRISMA) guidelines. The searched documents are gradually screened from the title, abstract, and full text according to the pre-set inclusion exclusion criteria. The two researchers conducted the same discussion at the same time. When there is controversy, it should be judged by the third researcher.

**Conflict of interests** The authors declare they have no conflict of interests.

## References


1. Sveinbjornsdottir S (2016) The clinical symptoms of Parkinson's disease. J Neurochem 139(Suppl 1):318–324
2. Niu XL, Liu L, Song ZX, Li Q, Wang ZH, Zhang JL, Li HH (2016) Prevalence of small intestinal bacterial overgrowth in Chinese patients with Parkinson's disease. J Neural Transm (Vienna) 123(12): 1381–1386
3. Zou YM, Liu J, Tian ZY, Lu D, Zhou YY (2015) Systematic review of the prevalence and incidence of Parkinson's disease in the People's Republic of China. Neuropsychiatr Dis Treat 11:1467–1472
4. Jankovic J (2008) Parkinson's disease: clinical features and diagnosis. J Neurol Neurosurg Psychiatry 79(4):368–376
5. Braak H, Ghebremedhin E, Rüb U, Bratzke H, Del Tredici K (2004) Stages in the development of Parkinson's disease-related pathology. Cell Tissue Res 318(1):121–134
6. Sweeney MD, Zhao Z, Montagne A, Nelson AR, Zlokovic BV (2019) Blood-brain barrier: from physiology to disease and back. Physiol Rev 99(1):21–78
7. Zucca FA, Vanna R, Cupaioli FA, Bellei C, de Palma A, di Silvestre D, Mauri P, Grassi S, Prinetti A, Casella L, Sulzer D, Zecca L (2018) Neuromelanin organelles are specialized autolysosomes that accumulate undegraded proteins and lipids in aging human brain and are likely involved in Parkinson's disease. NPJ Parkinsons Dis 4:17
8. Taniguchi D, Hatano T, Kamagata K, Okuzumi A, Oji Y, Mori A, Hori M, Aoki S, Hattori N (2018) Neuromelanin imaging and midbrain volumetry in progressive supranuclear palsy and Parkinson's disease. Mov Disord 33(9):1488–1492
9. Pavese N. 2018 Is neuromelanin the imaging biomarker for the early diagnosis of Parkinson's disease that we were looking for? *Parkinsonism Relat Disord.*
10. Rovini E, Maremmani C, Moschetti A, Esposito D, Cavallo F (2018) Comparative motor pre-clinical assessment in Parkinson's disease using supervised machine learning approaches. Ann Biomed Eng 46(12):2057–2068
11. Zhang Z, Wang J, Chen S, Liu C, Zhang B, Peng R, Sun S, Sun X, Zhao G, Qu Q, Li Y, Zhu S, Pan X, Shao M, Wang Y (2018) Efficacy and safety of rasagiline in Chinese patients with early Parkinson's disease: a randomized, double-blind, parallel, placebo-controlled, fixed-dose study. Transl Neurodegener 7:32
12. Emre M, Aarsland D, Brown R, Burn DJ, Duyckaerts C, Mizuno Y, Broe GA, Cummings J, Dickson DW, Gauthier S, Goldman J, Goetz C, Korczyn A, Lees A, Levy R, Litvan I, McKeith I, Olanow W, Poewe W, Quinn N, Sampaio C, Tolosa E, Dubois B (2007) Clinical diagnostic criteria for dementia associated with Parkinson's disease. Mov Disord 22(12):1689–1707 quiz 1837
13. Tarsy D, Gordon L 2012 Clinical diagnostic criteria for Parkinson's disease. In: Parkinson's disease. CRC Press, 732–741
14. Postuma RB, Berg D, Stern M, Poewe W, Olanow CW, Oertel W, Obeso J, Marek K, Litvan I, Lang AE, Halliday G, Goetz CG, Gasser T, Dubois B, Chan P, Bloem BR, Adler CH, Deuschl G (2015) MDS clinical diagnostic criteria for Parkinson's disease. Mov Disord 30(12):1591–1601
15. Hughes AJ, Daniel SE, Kilford L, Lees AJ (1992) Neurosurgery, Psychiatry. Accuracy of clinical diagnosis of idiopathic Parkinson's disease: a clinico-pathological study of 100 cases. J Neurol Neurosurg Psychiatry 55(3):181–184
16. El-Mewafy ZMH, Razek A, El-Eshmawy MM, El-Eneen NRA, El-Biaomy AAB (2018) Magnetic resonance spectroscopy of the frontal region in patients with metabolic syndrome: correlation with anthropometric measurement. Pol J Radiol 83:e215–e219
17. El-Serougy L, Abdel Razek AA, Ezzat A, Eldawoody H, El-Morsy A (2016) Assessment of diffusion tensor imaging metrics in

differentiating low-grade from high-grade gliomas. Neuroradiol J 29(5):400–407
18. Razek AA, Elmongy A, Hazem M, Zakareyia S, Gabr W (2011) Idiopathic Parkinson disease effect of levodopa on apparent diffusion coefficient value of the brain. Acad Radiol 18(1):70–73
19. Sasaki M, Shibata E, Kudo K, Tohyama K (2008) Neuromelanin-sensitive MRI. Clin Neuroradiol 18(3):147–153
20. Xing Y, Sapuan A, Dineen RA, Auer DP (2018) Life span pigmentation changes of the substantia nigra detected by neuromelanin-sensitive MRI. Mov Disord 33(11):1792–1799
21. Kostic VS, Agosta F, Petrovic I, Galantucci S, Spica V, Jecmenica-Lukic M, Filippi M (2010) Regional patterns of brain tissue loss associated with depression in Parkinson disease. Neurology 75(10): 857–863
22. Nakamura K, Sugaya K (2014) Neuromelanin-sensitive magnetic resonance imaging: a promising technique for depicting tissue characteristics containing neuromelanin. Neural Regen Res 9(7):759–760
23. Hashido T, Saito S (2016) Quantitative T1, T2, and T2* mapping and semi-quantitative neuromelanin-sensitive magnetic resonance imaging of the human midbrain. PLoS One 11(10):e0165160
24. Matsuura K, Maeda M, Yata K, Ichiba Y, Yamaguchi T, Kanamaru K, Tomimoto H (2013) Neuromelanin magnetic resonance imaging in Parkinson's disease and multiple system atrophy. Eur Neurol 70(1–2):70–77
25. Prasad S, Stezin A, Lenka A, George L, Saini J, Yadav R, Pal PK (2018) Three-dimensional neuromelanin-sensitive magnetic resonance imaging of the substantia nigra in Parkinson's disease. Eur J Neurol 25(4):680–686
26. Schwarz ST, Xing Y, Tomar P, Bajaj N, Auer DP (2017) In vivo assessment of brainstem depigmentation in Parkinson disease: potential as a severity marker for multicenter studies. Radiology 283(3):789–798
27. Kiebish MA, Narain NR (2019) Enabling biomarker discovery in Parkinson's disease using multiomics: challenges, promise and the future. Per Med 16(1):5–7
28. Zhang X, Gao F, Wang D, Li C, Fu Y, He W, Zhang J (2018) Tau pathology in Parkinson's disease. Front Neurol 9:809
29. Baquet ZC, Williams D, Brody J, Smeyne RJ (2009) A comparison of model-based (2D) and design-based (3D) stereological methods for estimating cell number in the substantia nigra pars compacta (SNpc) of the C57BL/6J mouse. Neuroscience 161(4):1082–1090
30. Yang J, Burciu RG, Vaillancourt DE (2018) Longitudinal progression markers of Parkinson's disease: current view on structural imaging. Curr Neurol Neurosci Rep 18(12):83
31. Knorle R (2018) Neuromelanin in Parkinson's disease: from Fenton reaction to calcium signaling. Neurotox Res 33(2):515–522
32. Matsuura K, Maeda M, Tabei KI, Umino M, Kajikawa H, Satoh M, Kida H, Tomimoto H (2016) A longitudinal study of neuromelanin-sensitive magnetic resonance imaging in Parkinson's disease. Neurosci Lett 633:112–117
33. Ohtsuka C, Sasaki M, Konno K, Koide M, Kato K, Takahashi J, Takahashi S, Kudo K, Yamashita F, Terayama Y (2013) Changes in substantia nigra and locus coeruleus in patients with early-stage Parkinson's disease using neuromelanin-sensitive MR imaging. Neurosci Lett 541:93–98
34. Reimao S, Pita Lobo P, Neutel D et al (2015) Quantitative analysis versus visual assessment of neuromelanin MR imaging for the diagnosis of Parkinson's disease. J Park Dis 5(3):561–567
35. Castellanos G, Fernandez-Seara MA, Lorenzo-Betancor O et al (2015) Automated neuromelanin imaging as a diagnostic biomarker for Parkinson's disease. Mov Disord 30(7):945–952
36. Takahashi H, Watanabe Y, Tanaka H et al (2018) Quantifying changes in nigrosomes using quantitative susceptibility mapping and neuromelanin imaging for the diagnosis of early-stage Parkinson's disease. Br J Radiol 91(1086):20180037
37. Isaias IU, Trujillo P, Summers P et al (2016) Neuromelanin imaging and dopaminergic loss in Parkinson's disease. Front Aging Neurosci 8:196
38. Ogisu K, Kudo K, Sasaki M, Sakushima K, Yabe I, Sasaki H, Terae S, Nakanishi M, Shirato H (2013) 3D neuromelanin-sensitive magnetic resonance imaging with semi-automated volume measurement of the substantia nigra pars compacta for diagnosis of Parkinson's disease. Neuroradiology 55(6):719–724